NMR Study of the Cold, Heat, and Pressure Unfolding of Ribonuclease A†

Jing Zhang,‡ Xiangdong Peng,‡ Ana Jonas,§ and Jiri Jonas*,‡

Department of Chemistry, School of Chemical Sciences, and Department of Biochemistry, College of Medicine, University of Illinois, Urbana, Illinois 61801

Received December 6, 1994; Revised Manuscript Received March 24, 1995⊗

ABSTRACT: The reversible cold, heat, and pressure unfolding of RNase A and RNase A−inhibitor complex were studied by 1D and 2D ^{1}H NMR spectroscopy. The reversible pressure denaturation experiments in the pressure range from 1 bar to 5 kbar were carried out at pH 2.0 and 10 °C. The cold denaturation was carried out at 3 kbar, where the protein solution can be cooled down to −25 °C without freezing. Including heat denaturation experiments, the experimental data obtained allowed us to construct the pressure−temperature phase diagram of RNase A. The experimental results suggest the possibility that all three denaturation processes (cold, heat, and pressure) lead to non-cooperative unfolding. The appearance of a new histidine resonance in the cold-denatured and pressure-denatured RNase A spectra, compared to the absence of this resonance in the heat-denatured state, indicates that the pressure-denatured and cold-denatured states may contain partially folded structures that are similar to that of the early folding intermediate found in the temperature-jump experiment reported by Blum et al. [Blum, A. D., et al. (1978) *J. Mol. Biol. 118*, 305]. A hydrogen-exchange experiment was performed to confirm the presence of partially folded structures in the pressure-denatured state. Stable hydrogen-bonded structures protecting the backbone amide hydrogens from solvent exchange were observed in the pressure-denatured state. These experimental results suggest that the pressure-denatured RNase A displays the characteristics of a molten globule. The cold, heat, and pressure denaturation experiments on the complex of RNase A with the inhibitor 3′-UMP show that the RNase A−inhibitor complex is more stable than RNase without the inhibitor.

Since Anfinsen and colleagues (Anfinsen, 1973) first studied the renaturation of reduced and unfolded ribonuclease A (RNase A),[1] much effort has been expended in attempting to understand the relationships between the amino acid sequence, the structure, and dynamic properties of the native conformation of proteins. Recently, increasing attention has been focused on denatured and partially folded states, since determination of their structure and stability may provide critical insights into the mechanisms of protein folding (Kim & Baldwin, 1990; Creighton, 1993; Matthias et al., 1994). The native conformations of hundreds of proteins are known in great detail from structural determinations by X-ray crystallography and, more recently, by NMR spectroscopy. However, detailed knowledge of the conformations of denatured and partially folded states is lacking, which is a serious shortcoming in current studies of protein stability and protein folding pathways (Robertson & Baldwin, 1991).

Most studies dealing with protein denaturation have been carried out at atmospheric pressure using various physicochemical perturbations, such as temperature, pH, or denaturants, as experimental variables. Compared to varying temperature, which produces simultaneous changes in both volume and thermal energy, the use of pressure to study protein solutions perturbs the environment of the protein in a continuous, controlled way by changing only intermolecular distances (Weber & Drickamer, 1983). In addition, by taking advantage of the phase behavior of water, high pressure can substantially lower the freezing point of an aqueous protein solution. Therefore, by applying high pressure, one can investigate in detail not only pressure-denatured proteins but also cold-denatured proteins in aqueous solution. There is yet another reason for systematic studies of the pressure unfolding of proteins related to the new theoretical approach by Bryngelson and Wolynes (1987, 1989, 1990), which uses statistical characterization of the energy landscape in analyzing protein folding. Bryngelson et al. (1994) pointed out the need for statistics involving different modes of denaturation and specifically indicated the advantages of high-pressure denaturation studies because pressure strongly affects all solvent-mediated interactions and may correlate with the roughness energy scale.

Cold denaturation has been assumed to be a general property of all globular proteins (Privalov, 1990; Antonino et al., 1991). However, experimental evidence for cold denaturation has been scant, due to the fact that cold denaturation of proteins in aqueous solution is usually observed only at temperatures below 0 °C at neutral pH. Different approaches have been utilized to prevent freezing of protein solutions, including the use of cryosolvents (Hatley & Franks, 1986), denaturants (Privalov, 1990), emulsions in oil (Franks & Hatley, 1985), and supercooled aqueous solutions (Hatley & Franks, 1986; Tamura et al., 1991).

† This work was supported by National Institutes of Health Grant No. PHS 5 RO1 GM 42452.

* Author to whom correspondence should be addressed.

‡ Department of Chemistry, School of Chemical Sciences.

§ Department of Biochemistry, College of Medicine.

⊗ Abstract published in *Advance ACS Abstracts,* June 15, 1995.

[1] Abbreviations: RNase A, bovine pancreatic ribonuclease A (type X11 A); pH*, pH meter reading (calibrated by reference to standard buffers in H_2O for samples dissolved in ^2H_2O and uncorrected for the deuterium isotope effect on the glass electrode); 1D, one-dimensional proton NMR spectroscopy, 2D, two-dimensional proton NMR spectroscopy; TSP, sodium salt of 3-(trimethylsilyl)propionic-*2,2,3,3-d*$_4$ acid; 3′-UMP, uridine 3′-monophosphate.

0006-2960/95/0434-8631$09.00/0

In this article, we illustrate the advantages of using high-pressure, high-resolution ^{1}H NMR techniques to study the reversible pressure, cold, and heat denaturation of RNase A. This work is a continuation of our systematic studies of pressure-induced unfolding of proteins (Samarasinghe et al., 1992; Peng et al., 1993, 1994; Royer et al., 1993) and has the following specific objectives: (1) to investigate the pressure unfolding of RNase A; (2) to characterize the structure of the pressure-denatured protein; and (3) to compare the unfolded structures of RNase A produced by cold, heat, and pressure denaturation.

RNase A is a single-domain protein, a pancreatic enzyme that catalyzes the cleavage of single-stranded RNA. This protein consists of 124 amino acid residues with a molecular mass of 13.7 kDa. It has traditionally served as a model for protein folding because it is small and stable and has a well-known native structure. The ϵ1 protons of the four RNase A histidine residues are well-resolved from other protons in the ^{1}H NMR spectrum of the native protein in D_2O; they have been used in this work to monitor the structural changes of four distinct segments in the molecule during cold, heat, and pressure denaturation processes. His12 and His119 are part of the catalytic site of native RNase A, and His48 is at the hinge of the active site crevice. His48, His105, and His119 are in the β-sheet fold, which forms the backbone of the molecule. His12 is in an α-helix near the N-terminus. The folding pathway of the protein has been studied extensively. Several studies on RNase A strongly suggest that its folding proceeds through intermediates, including an early hydrogen-bonded intermediate and a late native-like intermediate (Cook et al., 1979; Schmid & Baldwin, 1979; Kim & Baldwin, 1980; Schmid, 1983; Udgaonkar & Baldwin, 1988, 1990). Theoretical and experimental evidence suggests that nonrandom structures exist in the denatured protein. Circular dichroism (CD) and Fourier transform infrared (FTIR) data indicate that there is a significant amount of structure in thermally denatured RNase A (Labhardt, 1982; Seshadri & Fink, 1994), although a stable hydrogen-bonded structure could not be detected by amide proton protection experiments (Robertson & Baldwin, 1991).

In order to obtain specific structural information on the pressure-denatured RNase A, we used the hydrogen-exchange method. In this method, the exchangeable amide protons (NH) of a protein are used as probes of structure and structural changes. The NH proton exchange with solvent deuterons is strongly dependent on their involvement in stable hydrogen bonds. The observation of slowed amide exchange is a powerful and site-specific probe for detecting persistent structure in proteins (Englander et al., 1992; Matthias et al., 1994). Two-dimensional NMR spectroscopy can be used to determine the hydrogen-exchange rates of individual backbone amide protons of a protein. Schmid and Baldwin (1979) first introduced the ^{1}H$-^3$H exchange approach in their studies on the folding of ribonuclease A and found that at least part of the hydrogen-bonded backbone of RNase A is formed at an early stage in folding. Udgaonkar and Baldwin (1988, 1990) used pH pulse labeling to study refolding of RNase A; their results show very fast and very slow kinetic components and suggest that native-like secondary structures are present in early folding intermediates of RNase A.

MATERIALS AND METHODS

Bovine pancreatic ribonuclease A (type XII A) was purchased from Sigma Chemical Co. and used without further purification. For 1D ^{1}H NMR experiments, the protein was dissolved in D_2O at pH* 3, and the solution was heated to 60 °C for 20 min to allow deuterium exchange of the labile amide protons in RNase A; the sample was then lyophilized from D_2O. This procedure was performed twice for each sample. The uncorrected pH values of D_2O solutions were adjusted using DCl (Sigma) and NaOD (MSD Isotopes).

The deuterated RNase A was dissolved to a concentration of 4 mM in 20 mM maleic acid buffer and 0.3 M NaCl in 99.9% D_2O, adjusting the pH* to 2.0. The pK_a of maleic acid buffer is insensitive to pressure, and the effective pH of the solutions is only changed by about 0.3 pH unit for the highest pressure (5.25 kbar) used in the experiment (Kitamura & Itoh, 1987). The change is not expected to affect the overall denaturation of the enzyme significantly, compared to pressure denaturation. In addition, the pK_a of the histidine residues is insensitive to pressure changes (Zipp & Kauzmann, 1973). The enzymatic activity of RNase A was determined before and after compression by the spectrophotometric assay using cytidine 2′,3′-phosphate (Sigma), as described in the literature (Crook et al., 1960). The results of both NMR spectra and enzymatic assays indicate that the heat, cold, and pressure denaturation of RNase A were completely reversible. For the RNase A−inhibitor experiment, a sample was prepared containing 4 mM deuterated RNase A and 12 mM uridine 3′-monophosphate (3′-UMP Sigma) in 20 mM maleic acid buffer and 0.3 M NaCl in 99.9% D_2O at pH* 3.0. The control RNase A sample was prepared in exactly the same way, except that no 3′-UMP was added.

In the high-pressure experiments, the enzyme solution was loaded into a special glass sample cell. The sample cell is equipped with a movable Teflon piston that can transmit the liquid pressure in the high-pressure vessel to the sample solution. CS_2 is used as the pressurizing fluid. The pressure was generated by a hand-operated hydraulic system and measured with a Heise pressure gauge. The temperature was controlled by circulating ethylene glycol/water through a thermostating jacket around the pressure vessel and monitored by a copper/constantan thermocouple located inside the vessel near the sample cell. The lower temperatures (<-10 °C) were attained with a refrigerated bath (Brinkmann Co.) circulating methanol. The detailed design of the high-pressure setup has been described previously (Jonas, 1987).

The pressure denaturation experiments on RNase A were carried out at pH* 2.0 and 10 °C. The pressure denaturation of the RNase A−inhibitor complex and the control experiment (RNase A only) were carried out at pH* 3.0 and 20 °C. Under these conditions, the protein is completely folded at 1 bar. The cold denaturation of RNase A was carried out at 3 kbar, where the protein solution can be cooled down to −25 °C without freezing. All 1D ^{1}H NMR data were obtained on a General Electric GN300 spectrometer operating at a proton frequency of 300 MHz. The spectra were collected using a 5000 Hz spectral width, 128 scans, a 60° pulse width, and a 2 s recycle delay. Each FID was composed of 8192 data points. The spin−lattice relaxation time measurements were performed using the inversion−recovery method (180°−τ−190°) with delay times longer

than $5T_1$. Before each measurement, the sample was allowed to equilibrate to the specific pressure and temperature. For the determination of reaction volumes for the various histidines, the integration procedure was as follows. A 60° pulse width was used, with a 2 s delay time and an acquisition delay of 0.82 s. T_1 for the native state is always much smaller than 1 s ($T_1 \cong 0.6$ s), and within experimental error the native state T_1 does not change with pressure. The integration experiments were repeated with different acquisition parameters, and the results obtained agreed within experimental error. For the actual determination of the reaction volumes ($\Delta V°$), four independent experiments were carried out. The values given in the text represent the means of the four measurements and their standard deviations.

For the hydrogen-exchange experiments, the RNase A samples were prepared as follows: first, RNase A powder was dissolved to a concentration of 4 mM in 20 mM maleic acid buffer and 0.2 M NaCl in 99.9% D_2O, adjusting the pH* to 2.0. Then, the freshly prepared RNase A solution was loaded into the sample cell, and the cell was placed in the high-pressure vessel at ambient pressure at 5 °C. Under these conditions, the protein is in its native state. The sample was pressurized to 4.2 kbar at 10 °C, where the RNase A was completely pressure-denatured. After staying in the pressure-denatured state for a time of 0−50 min, the sample was depressurized to ambient pressure. The protein solution was removed from the sample cell, and the pH* was adjusted to 3.0. Finally, the RNase A solution was loaded into a 5 mm NMR tube, and the absolute value mode $^1H-^1H$ COSY spectra were recorded at a temperature of 30 °C.

The 2D homonuclear *J*-correlated (COSY) spectra (Aue et al., 1976) were obtained on a Varian VXA 500 spectrometer operating at a proton frequency of 500 MHz. The data sets consist of 512 blocks of t_1, 16 summed scans for each t_1 block, and 1024 complex data points in t_2. The spectral width was 7000 Hz and the recycle delay was 1.5 s. The 2D COSY data were processed using Felix 2.05 software on a Silicon Graphics workstation. The cross-peak intensities were measured and normalized to the sum of the intensities of the nonexchangeable aromatic resonances. All chemical shifts were referenced to an internal standard of sodium 3-(trimethylsilyl)propionate-*2,2,3,3-d*$_4$ (TSP). The accuracy of the temperature measurement was ±0.2 °C, and the accuracy of the pressure measurements was ±0.02 kbar.

RESULTS

Pressure Denaturation of RNase A. The ϵ1 protein peaks of the four histidine residues are well-resolved from other proton peaks in the 1D ^1H spectrum of the native RNase A in D_2O. They have been assigned and used to probe the folding and unfolding processes of the protein. Figure 1 shows the behavior of the proton spectrum in the histidine region during pressure unfolding at pH* 2.0 and 10 °C. With increasing pressure, the intensity of the native histidine peak decreases. At about 4 kbar, all native histidine resonances diappear, indicating that the protein is pressure-denatured. As the pressure increases, two denatured resonances of the histidine residues, D and D′, are observed. The chemical shift of resonance D is very similar to the composite resonance observed in the thermally denatured state and in the urea- or guanidine hydrochloride-denatured states of the protein (Westmoreland & Matthews, 1973; Benz & Roberts, 1975a,b). The interesting feature in the pressure unfolding

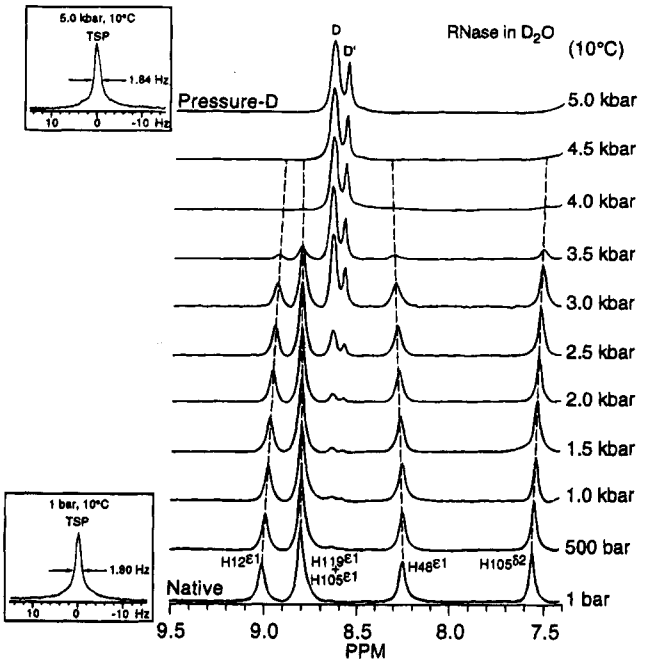

FIGURE 1: Histidine region of the ^1H NMR spectra of RNase A in D_2O at various pressures (10 °C, pH* 2.0). The standard in the insets is sodium 3-(trimethylsilyl)tetradeuteriopropionate.

process is that, besides the composite denatured histidine resonance D, another denatured histidine resonance, D′, appears as the pressure increases. This resonance was not observed in either the thermal denatured state or the urea- or guanidine hydrochloride-denatured states. In the completely pressure-denatured state, the intensity ratio of D to D′ is 3:1, suggesting that D′ comes from one of the four histidine residues. In order to assign the D′ resonance, a magnetization transfer NMR experiment (Dobson & Evans, 1984; Evans et al., 1989) was performed. It was found that the intensity of resonance D′ decreased when the native histidine 12 peak was selectively irradiated. The results of the magnetization transfer test indicate that resonance D′ comes from histidine 12 and that resonance D comes from histidines 48, 105, and 119. We also found in the magnetization transfer experiment that the exchange rate between the native state and the pressure-denatured state of RNase A is much slower than that of lysozyme (Dobson & Evans, 1984; our unpublished results). The identical chemical shifts of the three pressure-denatured histidines in the composite resonance D suggest that they are in equivalent environments. The difference in chemical shift of the His12 resonance compared to the resonances of the other three histidines in the pressure-denatured state implies that His12 is in a different environment than the other three.

It is interesting to note that the extra denatured histidine peak (D′) resembles a similar peak in the temperature-jump refolding experiment of Blum et al. (1978). In that kinetic study of the refolding of heat-unfolded RNase A, the extra denatured resonance (X) was assigned to His12 in a folding intermediate in which His12 is in a partly folded environment. Another denatured resonance (U) was assigned to the other three residues, which are in unfolded environments. The relative chemical shift positions of D and D′ in this pressure denaturation experiment are the same as those of U and X in the temperature-jump refolding experiment. The appearance of new histidine resonances was also reported in the refolding study of RNase A in aqueous methanol

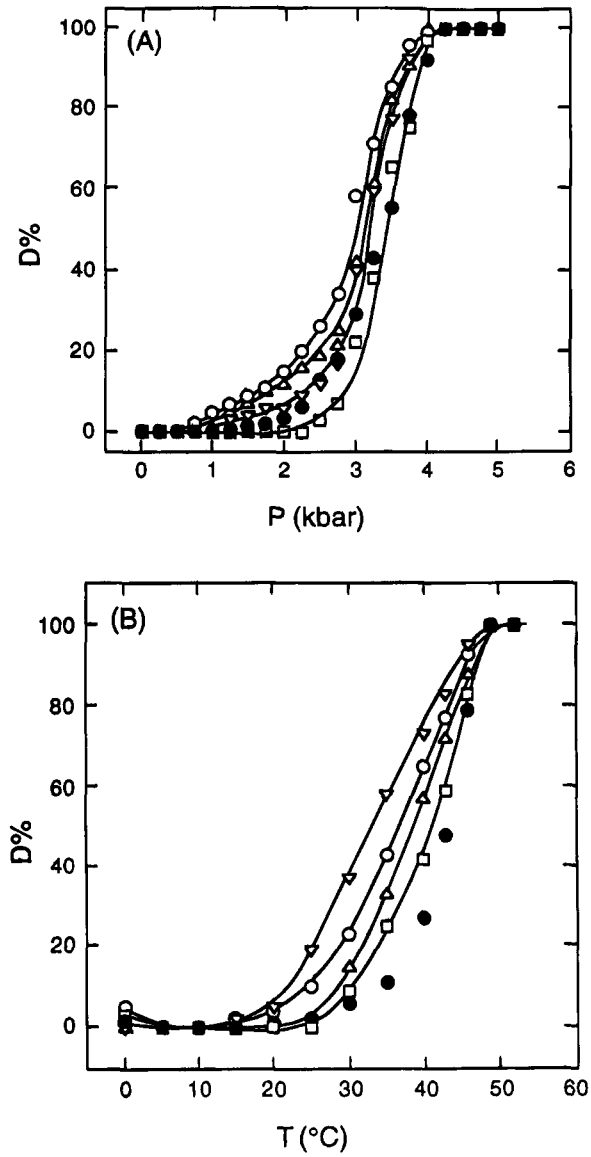

FIGURE 2: (A) Pressure denaturation curves for histidine residues obtained from NMR spectra at 10 °C, pH* 2.0. (B) Temperature denaturation curves for histidine residues obtained from NMR spectra at ambient pressure, pH* 2.0 (○, His12$^{\epsilon 1}$; △, His48$^{\epsilon 1}$; ▽, His119$^{\epsilon 1}$ + His105$^{\epsilon 1}$; □, His105$^{\delta 2}$; ●, D + D′).

cryosolvents in the subzero temperature range (Biringer & Fink, 1982).

From Figure 1, one can also see that the chemical shifts of histidines in both native and denatured states change only slightly with pressure. Under high pressure, the chemical shift of the composite denatured resonance D of the three histidine residues (His48, His105, and His119) agrees with the average chemical shift of these residues. In addition, the chemical shifts of the native and denatured histidine resonances measured as a function of temperature at ambient pressure were also insensitive to temperature.

The percent denaturation of each histidine residue was calculated and plotted as a function of pressure in Figure 2A. The percent denaturation of each histidine residue was obtained from the integrated areas of the native resonances. For each spectrum, the integrated area of the standard TSP resonance was used as the internal intensity standard. The intensity of the native resonance for each histidine residue at ambient pressure was chosen as 100% of the native state proton signal. In order to compare the pressure denaturation process to the thermal denaturation process, the thermal denaturation experiment of RNase A at ambient pressure was performed under the same solution conditions, and the percent thermal denaturation of each histidine residue is plotted in Figure 2B. The results of the thermal denaturation at ambient pressure are consistent with those reported earlier (Westmoreland & Matthews, 1973; Benz & Roberts, 1975a,b). It should be noted that the assignment of His12 and His119 in these papers has been corrected by Petal et al. (1975). The van't Hoff enthalpy $\Delta H°$ from the denatured histidine peaks is 66 ± 5 kcal/mol, which compares closely with the value of 65 kcal/mol determined by thermocalorimetry (Tsong et al., 1970) and 70 kcal/mol by NMR (Westmoreland & Matthews, 1973). The $\epsilon 1$ histidine resonances of His119 and His105 overlap, which makes it more difficult to analyze their behavior separately. However, the $\delta 2$ proton resonance of His105 is well-resolved, as shown in Figure 1, and can be used to calculate the denaturation curve of His105. From Figure 2, it can easily be seen that, for both the pressure and thermal denaturation processes, each histidine residue follows a different denaturation curve, suggesting non-cooperativity of these processes. By comparing the denaturation curves in Figure 2A,B, it is clear that the behavior of the pressure denaturation of histidine residues is different from that of their thermal denaturation.

We want to point out that the denaturation curves for the individual residues represent average values obtained from four independent experiments. Due to the limits in experimental accuracy in the determination of the extent of denaturation at each pressure, we cannot interpret these experimental results as unambiguous proof that the unfolding process is not cooperative. Nevertheless, we can describe, in a phenomenological sense, the trends in the experimental denaturation curves for individual histidine residues. In the pressure denaturation (Figure 2A), the intensity of the His12 resonance begins to decrease before other histidines, and it decreases more rapidly with increasing pressure. On the other hand, one can see that His105 does not unfold until the pressure is close to 2 kbar, and it unfolds after the other histidine residues. The order of unfolding of the histidines with increasing pressure is His12, His48, His119, and His105. The percentage curve of D + D′ in Figure 2A was obtained from the integrated areas of the two denatured resonances D and D′. The sum of the integrated areas of the denatured resonances at 5 kbar of pressure was chosen as 100% of proton occupancy of the pressure-denatured state.

Since the four histidines are located in different regions of the molecule, it is interesting to determine the pressure effects on the denaturation processes of the individual histidine residues by calculating the reaction volume of each histidine. By assuming a two-state model, the reaction volumes ($\Delta V°$) can be obtained according to the following equation (Weber & Drickamer, 1983):

$$\left(\frac{\partial(\ln K_p)}{\partial P}\right)_T = -\frac{\Delta V°}{RT} \quad (1)$$

where $\Delta V°$ is the reaction volume, P is the pressure, and T is the temperature. The equilibrium constant for denaturation (K_p) is calculated from the primary data as follows:

$$K_p = \frac{I_o - I_p}{I_p} \quad (2)$$

where I_p and I_o are the intensities of the native resonances at pressure P and ambient pressure, respectively. The reaction volumes, $\Delta V°$, for the histidine residues of RNase A were calculated and represent means of four independent experiments with the standard deviation given. The $\Delta V°$ values for His12$^{\epsilon 1}$, His48$^{\epsilon 1}$, His119$^{\epsilon 1}$ and His105$^{\epsilon 1}$, and His105$^{\delta 2}$ are -53 ± 4, -61 ± 5, -42 ± 3, and -73 ± 7 mL/mol, respectively. The $\Delta V°$ value calculated from the denatured histidine resonance peaks (D + D′), -59 ± 5 mL/mol, is in good agreement with the literature value of -58 mL/mol determined by an optical method (Brandts et al., 1970). By using the analysis of variance, one may conclude that the differences in the $\Delta V°$ values reported are statistically significant within a 5% limit ($P = 0.05$). However, if one eliminates the $\Delta V°$ value for the overlapped peak for residues His119$^{\epsilon 1}$ + His105$^{\epsilon 1}$, then the analysis of variance calculation shows that the differences in $\Delta V°$ values are not statistically significant within a 5% limit ($P = 0.05$). The physical basis for the volume change for protein denaturation is highly complex; it involves, at least, contributions from compressibility, exposure of hydrophobic residues in the native and denatured states, and free volume in the native state. From the data available at present, it is not possible to evaluate the relative contributions of these effects to experimental $\Delta V°$ (Royer et al., 1993). In addition, as found in this experiment, the pressure denaturation of RNase A does not appear to be a single-step process. Therefore, the reaction volumes calculated from eq 1 can only be used in a phenomenological way to analyze the experimental data, and any interpretation of the volume change should be made with caution. Nevertheless, in spite of the fact that we used a two-state model assumption to calculate $\Delta V°$ values, the differences in ΔV° values for individual histidines suggest a multistep process.

Pressure-Assisted Cold and Heat Denaturation of RNase A. It is difficult to attain the completely cold-denatured state of proteins in aqueous solutions by decreasing the temperature below the freezing point of 0 °C at ambient pressure. However, taking advantage of the pressure phase behavior of water (Jonas, 1982), one can lower the temperature of aqueous solutions well below 0 °C. At 3 kbar the RNase A solution, as described in Materials and Methods, can be cooled to −25 °C without freezing. It should be noted here that the protein solution in the high-salt buffer freezes well below the freezing point given in the phase diagram of water at 3 kbar (−15 °C) (Jonas, 1982). The phase behavior of water allows us to obtain the completely cold-denatured state of RNase A with the assistance of pressure. In Figure 3, we demonstrate the behavior of the proton spectrum of the histidine region of RNase A undergoing both cold and heat denaturation at 3 kbar and pH* 2.0. The protein becomes cold-denatured at −22 °C and heat-denatured at 40 °C. In the cold-denatured state, one finds, in addition to the composite resonance D, another resonance D′, which likely has the same origin as D′ in the pressure-denatured state. This is not surprising because the protein is subjected to both a high pressure of 3 kbar and low temperature. The line width broadening of resonances D and D′ is due to slower motions at low temperatures. For the heat-denatured state at 3 kbar, the features of the double-denatured histidine peaks (denoted D_1 for the right and D_2 for the left) are similar to those of the heat-denatured state at ambient pressure, indicating that the heat-denatured protein is not a random

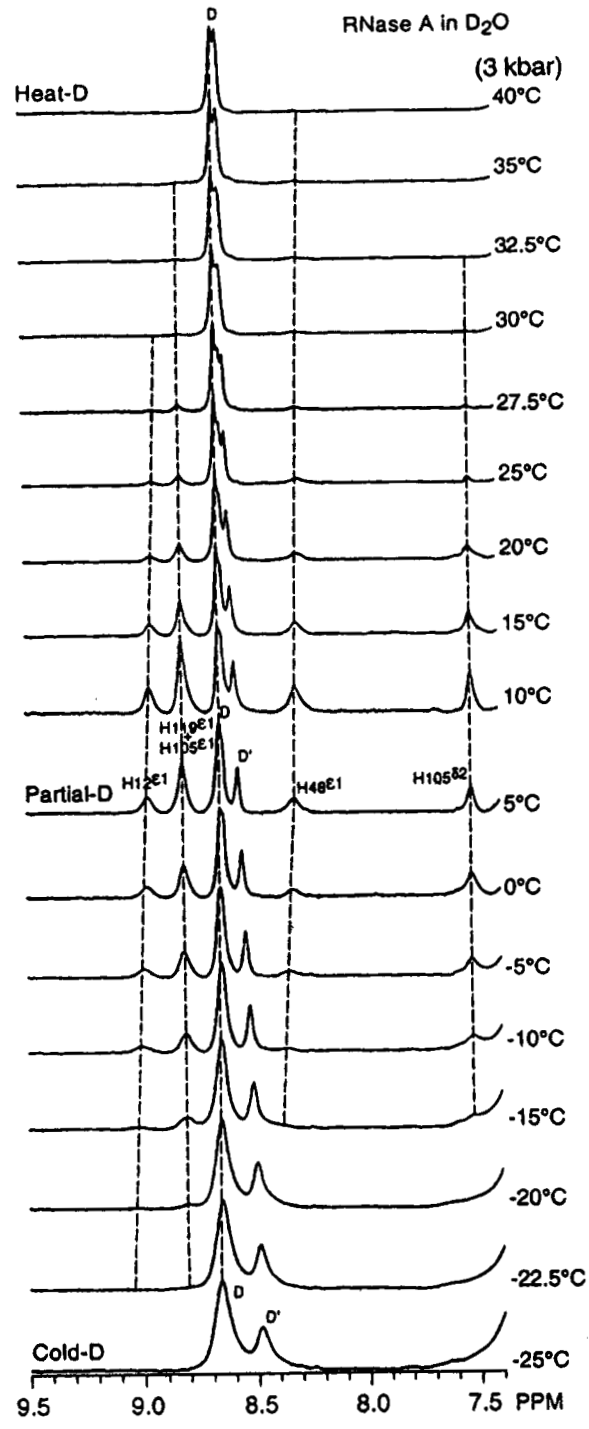

FIGURE 3: Histidine region of the ^{1}H NMR spectra of RNase A in D_2O at various temperatures (3 kbar, pH* 2.0).

coil structure. The percent temperature denaturation of each histidine residue at 3 kbar was calculated and plotted as a function of temperature in Figure 4, which shows the general trend in the temperature denaturation at 3 kbar. Again, we detect some indication of differences in the denaturation behavior of the individual histidine residues, but in view of limited experimental accuracy, we cannot conclude with certainty that the cold and heat denaturations of RNase A at 3 kbar represent non-cooperative processes.

In order to investigate the structural differences between the cold-denatured state and the heat-denatured state at 3 kbar, the chemical shifts of denatured histidine residues D and D′ were measured and plotted along with native histidine residue resonances as a function of temperature in Figure 5.

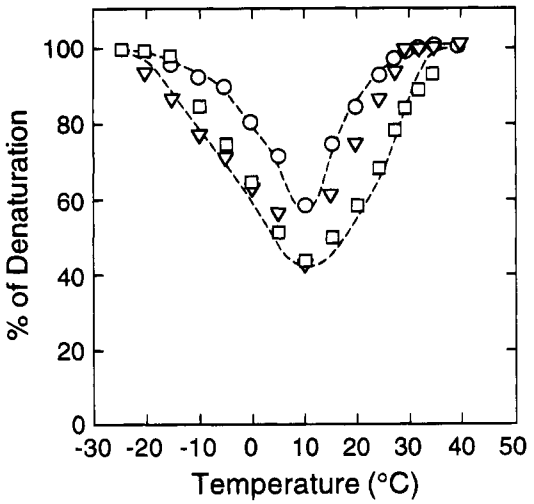

FIGURE 4: Temperature denaturation curves for histidine residues obtained from NMR spectra at 3 kbar of pressure, pH* 2.0. Experimental points for individual histidine residues: ○, His12$^{\epsilon 1}$; □, His48$^{\epsilon 1}$; ▽, His119$^{\epsilon 1}$ + His105$^{\epsilon 1}$.

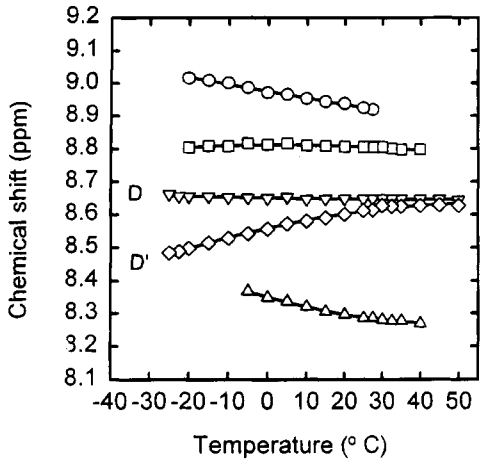

FIGURE 5: Temperature dependence of the chemical shifts of the histidine residues at 3 kbar, pH* 2.0 (○, His12$^{\epsilon 1}$; □, His119$^{\epsilon 1}$ + His105$^{\epsilon 1}$; ▽, D (His48 + His105 + His119); ◇, D′ (His12); △, His48$^{\epsilon 1}$).

It can be seen that the chemical shift of the composite denatured histidine residue D remains almost the same from the cold-denatured state to the heat-denatured state (−25 to 50 °C). This result implies that the chemical environments of the denatured residues of His48, His105, and His119 do not change significantly from the completely cold-denatured state to the heat-denatured state. However, the chemical shift of the denatured resonance D′ changes from the relatively large downfield shift in the cold-denatured state to the position close to the D resonance in the heat-denatured state. As in the pressure denaturation experiment, this chemical shift analysis provides evidence that the cold-denatured His12 residue is in a more folded environment, and the partially folded structure begins to unfold with increasing temperature until heat denaturation occurs, where His12 attains an environment similar to that of other histidines. This result agrees with the ^{1}H studies of the cold and heat denaturations of *Streptomyces* subtilisin inhibitor (Tamura et al., 1991), which showed that there is much less structure in the heat-denatured state than in the cold-denatured state. Figure 6 demonstrates that the chemical shifts of resonances D and D′ change with temperature at 5 kbar. The protein is completely denatured at 10 °C and 5 kbar. Resonance D is a doublet (D_1 and D_2) in the temperature-denatured state. It

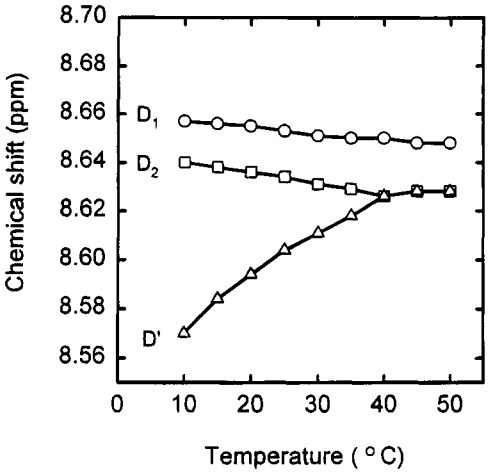

FIGURE 6: Temperature dependence of the chemical shifts of the denatured histidine resonances D (doublet D_1 and D_2) and D′ at 5 kbar.

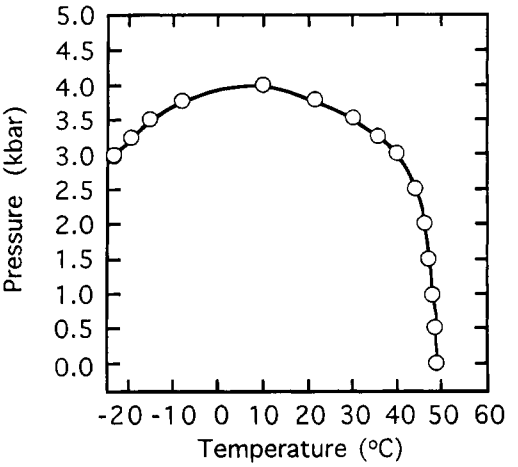

FIGURE 7: Phase diagram of RNase A at pH* 2.0.

can be seen in Figure 6 that, when temperature increases, resonance D′ shifts toward resonance D, and at about 40 °C resonance D′ merges into the D_2 peak of resonance D. At that point the protein enters the completely heat-denatured state.

Figure 7 shows the pressure−temperature phase diagram of RNase under the solution conditions described in Materials and Methods. Above the curve the protein is in the denatured state. It can be seen that the cold and heat denaturation temperatures change with pressure and that below 2 kbar the heat denaturation temperature is not sensitive to pressure. The cold denaturation temperature data below 3 kbar are not available because the aqueous protein solution freezes before it can be completely cold-denatured.

We also observed that all 1D ^{1}H spectra of the heat-denatured protein at different pressures (1 bar to 5 kbar) have almost the same appearance. This suggests that the heat-denatured states in the pressure range of this experiment have similar structures. However, for the cold-denatured states the complete proton spectra (not shown) at different pressures are much different. It appears that at lower pressure the cold-denatured protein may have more folded or partially folded structures than at higher pressures since the chemical shift difference between the D and D′ resonances decreases with increasing pressure.

Cold, Heat, and Pressure Denaturation of RNase A and the Inhibitor Complex. Since substrates or inhibitors stabilize native protein structures, it is interesting to use the histidine

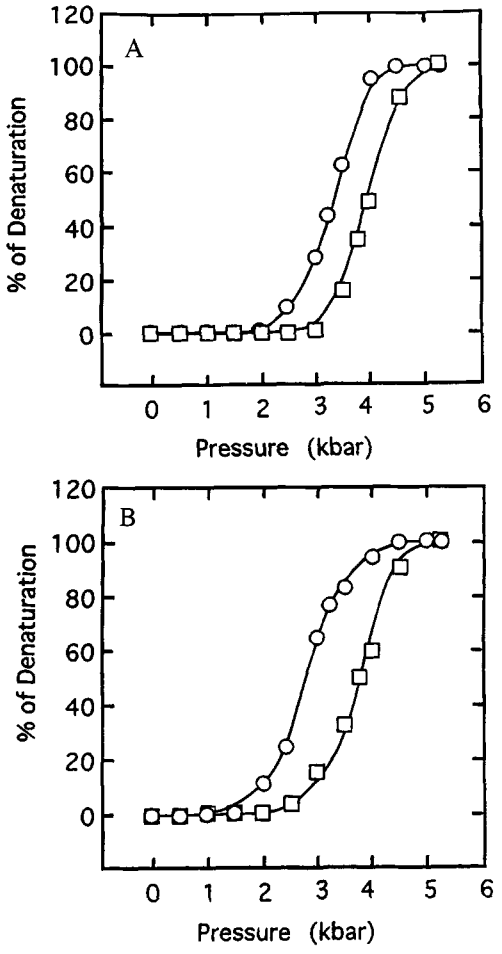

FIGURE 8: Comparison of the pressure denaturation curves of the RNase A protein only and the RNase A−inhibitor complex at 20 °C, pH* 3.0: (A) His48$^{\epsilon 1}$; (B) His105$^{\delta 2}$ (○, protein only; □, protein−inhibitor complex).

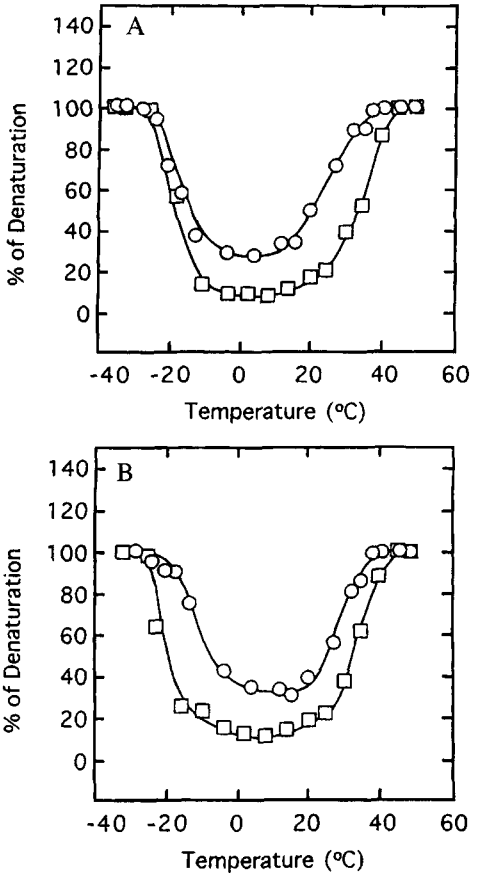

FIGURE 9: Comparison of the temperature denaturation curves of the RNase A protein only and the RNase A−inhibitor complex at 3 kbar, pH* 3.0: (A) His48$^{\epsilon 1}$; (B) His105$^{\delta 2}$ (○, protein only; □, protein−inhibitor complex).

residues of RNase A to probe the behavior of an enzyme−inhibitor complex under cold, heat, and pressure denaturation conditions. It is known that His12 and His119 are involved in enzymatic activity. The cold, heat, and pressure denaturations of the RNase A−inhibitor complex were investigated in this study by comparison to the denaturation of RNase A without the inhibitor. The competitive inhibitor 3′-UMP was used at a molar ratio of 3′-UMP to RNase A of 3:1. The native histidine 12 resonance is shifted upfield by about 0.09 ppm by the addition of 3′-UMP at pH* 3.0, 20 °C, and ambient pressure, indicating that the inhibitor is near the His12 residue on the enzyme. The chemical shifts of other histidine resonances are unaffected. The addition of the inhibitor does not change the chemical shifts of the denatured histidine resonances, indicating that the denatured protein does not bind the inhibitor. Due to the upfield shift of the native His12 resonance, the proton peak of His12 partly overlaps the peaks of His105 and His119. Therefore, it is difficult to accurately determine the denaturation effect of pressure and temperature for His12.

In Figure 8, the percent pressure denaturation of His48$^{\epsilon 1}$ and His105$^{\delta 2}$ of the enzyme−inhibitor complex and that of the enzyme without inhibitor under identical solution conditions are plotted separately as a function of pressure. It can be seen that the enzyme−inhibitor complex is more stable under pressure and therefore denatures later than the free enzyme. This is also true for the cold and heat denaturations shown in Figure 9, where the percent denaturation of His48 and His105 of RNase A with and without inhibitor at 3 kbar of pressure and pH* 3.0 is plotted as a function of temperature.

Hydrogen Exchange in the Pressure-Denatured State of RNase A. Since the simple appearance of resonance D′ does not allow one to arrive at unambiguous conclusions about the presence or absence of secondary structure in the pressure- and/or cold-denaturated states, we decided to carry out hydrogen-exchange experiments to test for the presence of partially folded structures in the pressure-denatured state. The hydrogen-exchange behavior contains information about the structural and conformational dynamics of proteins resolved to the level of individual amino acid residues. The protection against exchange of the amide proton of each amino acid residue imposed by the protein structure is expressed by the protection factor, $P = k_{rc}/k_{obs}$, where k_{rc} is the hydrogen-exchange rate calculated using a random coil model and k_{obs} is the hydrogen-exchange rate measured experimentally. In aqueous solutions, the rate of exchange of the peptide group NH proton with protons of the aqueous solvent is catalyzed by hydroxide and hydronium ions in pH-dependent reactions and by water in a pH-independent way (Bai et al., 1993). The random coil hydrogen-exchange rate can be expressed by

$$\begin{aligned} k_{rc} &= k(\text{acid}) + k(\text{base}) + k(\text{water}) \\ &= k_A[D^+] + k_B[OD^-] + k_W \\ &= k_A 10^{-pD} + k_B 10^{pD-pK_D} + k_W \end{aligned} \quad (3)$$

The random coil exchange rate is the sum of the contributions

from acid-, base-, and water-catalyzed exchanges, where k_A, k_B, and k_W are the respective rate constants. K_D is the D_2O dissociation constant, and $pK_D = -15.65$ at 5 °C (Covington et al., 1966). pD should be corrected for the pH meter anomaly in D_2O ($pD_{corr} = pD_{read} + 0.4$) (Glason & Long, 1960). The rate constants k_A, k_B, and k_W of individual residues of unfolded proteins are sensitive to neighboring side chains and can be calculated from the reference rates for alanine-containing peptides by considering the additivity of nearest-neighbor blocking and inductive effects.

The recently revised and extended parameters (Bai et al., 1993) were used to calculate the intrinsic exchange rates. To obtain the random coil exchange rates at a particular temperature and pressure, each rate constant in eq 3 should be modified according to

$$k_i(T,P) = k_i(T_0,P_0)\exp\left(-\frac{E_a}{R}\left(\frac{1}{T}-\frac{1}{T_0}\right)\right)\exp\left(-\frac{\Delta V^{\ddagger}(P-P_0)}{RT}\right) \quad (4)$$

where i = A, B, or W. E_a is the activation energy, and $\Delta V^{\ddagger}$ is the activation volume for hydrogen exchange. The activation energies (Bai et al., 1993) are $E_a(k_A)$ = 14 kcal/mol, $E_a(k_B)$ = 17 kcal/mol, and $E_a(k_W)$ = 14 kcal/mol; the activation volumes (Carter et al., 1978) are $\Delta V^{\ddagger}(k_A) = 0 \pm 1$ mL/mol, $\Delta V^{\ddagger}(k_B) = 6 \pm 1$ mL/mol, and $\Delta V^{\ddagger}(k_W) = -20.4$ mL/mol. These values were used to predict the hydrogen-exchange rates of individual residues of RNase A in a random coil structure at high pressure. The experimental hydrogen-exchange rate k_{obs} was obtained by fitting the measured cross-peak intensities to the exponential function, $I = I_0 \exp(-kt)$. The data measured at eight experimental times were used to obtain the experimental hydrogen-exchange rates at high pressure.

The cross-peaks between the NH and $C^{\alpha}H$ hydrogens of residues of RNase A in two-dimensional COSY NMR spectra were assigned according to the literature (Rico et al., 1989; Robertson et al., 1989). Of 119 backbone NHs in RNase A, approximately 40 amide protons are stable to exchange with D_2O in the native state, and they can be recorded by a COSY NMR spectrum. Only 33 of the 40 amide protons show cross-peaks of sufficient intensity to allow determination of the exchange rate in the pressure-jump experiment described in the Materials and Methods, and they are used to probe the stable hydrogen-bonded structure in the pressure-denatured protein. The individual rates of exchange can be determined from the spectra of various exchange-out periods for these amide protons. The experimental hydrogen-exchange rates of individual residues in RNase A, k_{obs}, in the pressure-denatured state, at 4.2 kbar, 10 °C, and pH* 2.0, are shown in Table 1. The predicted hydrogen-exchange rates for the corresponding residues, calculated from the random coil model at the experimental conditions, are also given in Table 1. The protection factors for the exchange of the measurable amide protons in the pressure-denatured state of RNase A at pH* 2.0 and 10 °C *versus* the protein sequence were plotted in Figure 10A. As a comparison, the protection factors *versus* the protein sequence in the heat-denatured state (Robertson & Baldwin, 1991) were also plotted in Figure 10B, showing that for the heat-denatured RNsae A there is no significant protection for any of the NH protons. One can see in Figure 10A that there are 8 residues with protection factors between 5 and 10 and 14 residues with protection factors larger than 10. These results provide further evidence that the pressure-denatured RNase A retains significant amounts of the native-like secondary structure.

Table 1: Amide Proton Exchange Rates and Protection Factors in Pressure-Denatured RNase A at 4.2 kbar, 10 °C

residue	$k_{obs} \times 100$ (min^{-1})	$k_{rc} \times 100$ (min^{-1})	P
Met13	9.4	150	16
Met29	10	36.1	3.6
Lys31	2.0	37.9	14
Val43	0.80	3.74	4.7
Asn44	12	51.7	4.3
Phe46	4.0	21.6	5.4
Val47	3.3	5.82	1.8
Glu49	11	266	24
Val54	1.3	19.2	15
Val57	6.3	6.28	1.0
Cys58	6.9	69.5	10
Ser59	3.4	189	56
Val63	1.7	10.7	6.3
Cys72	2.6	198	76
Tyr73	5.4	44.3	8.2
Gln74	16	30.4	1.9
Met79	1.8	35.7	20
Ile81	0.63	8.86	14
Thr82	2.6	11.7	4.5
Asp83	10	175	18
Cys84	4.7	376	80
Arg85	3.4	97.0	29
Thr87	3.6	47.9	13
Lys98	4.0	24.2	6.0
Thr100	5.2	30.9	5.9
Ala102	8.3	41.0	4.9
Lys104	8.0	44.9	5.6
Ile06	0.67	28.7	43
Ile107	3.0	2.78	0.93
Val108	0.92	3.10	3.4
Glu111	5.3	140	26
Val116	0.87	5.80	6.7
Val118	3.8	3.7	0.97

DISCUSSION

Previous thermal equilibrium studies of the reversible unfolding and folding of RNase A using NMR have provided evidence for the presence of intermediates in denaturation at low pH values (Westmoreland & Matthews, 1973; Benz & Roberts, 1975a,b). It was observed that the different regions of the protein do not unfold simultaneously. His119 unfolds first. Later, His12 begins to change, followed by His48, and His105 unfolds last. Benz and Roberts (1975a,b) indicated that the intermediates detected in the thermal unfolding at low pH are apparently the same as the intermediates induced by urea or guanidinium hydrochloride. A ^{13}C NMR study of the thermal unfolding of RNase A by Howarth (1979) gave further evidence for the existence of partially folded intermediates during unfolding. This study of RNase A pressure unfolding suggests that different regions of the protein do not unfold cooperatively. During pressure denaturation, it was found that His12 unfolds first but retains a partially folded environment, even in the completely pressure-denatured states. His48 begins to unfold after His12. This suggests that unfolding of the His12 region may affect the environment of His48 and may promote unfolding of the His48 region. His105 unfolds after the other histidines during pressure denaturation, which is similar to the thermal denaturation and the denaturation induced by urea or guanidine hydrochloride. A possible pathway for pressure unfolding of RNase A is the following: the N-terminal helix

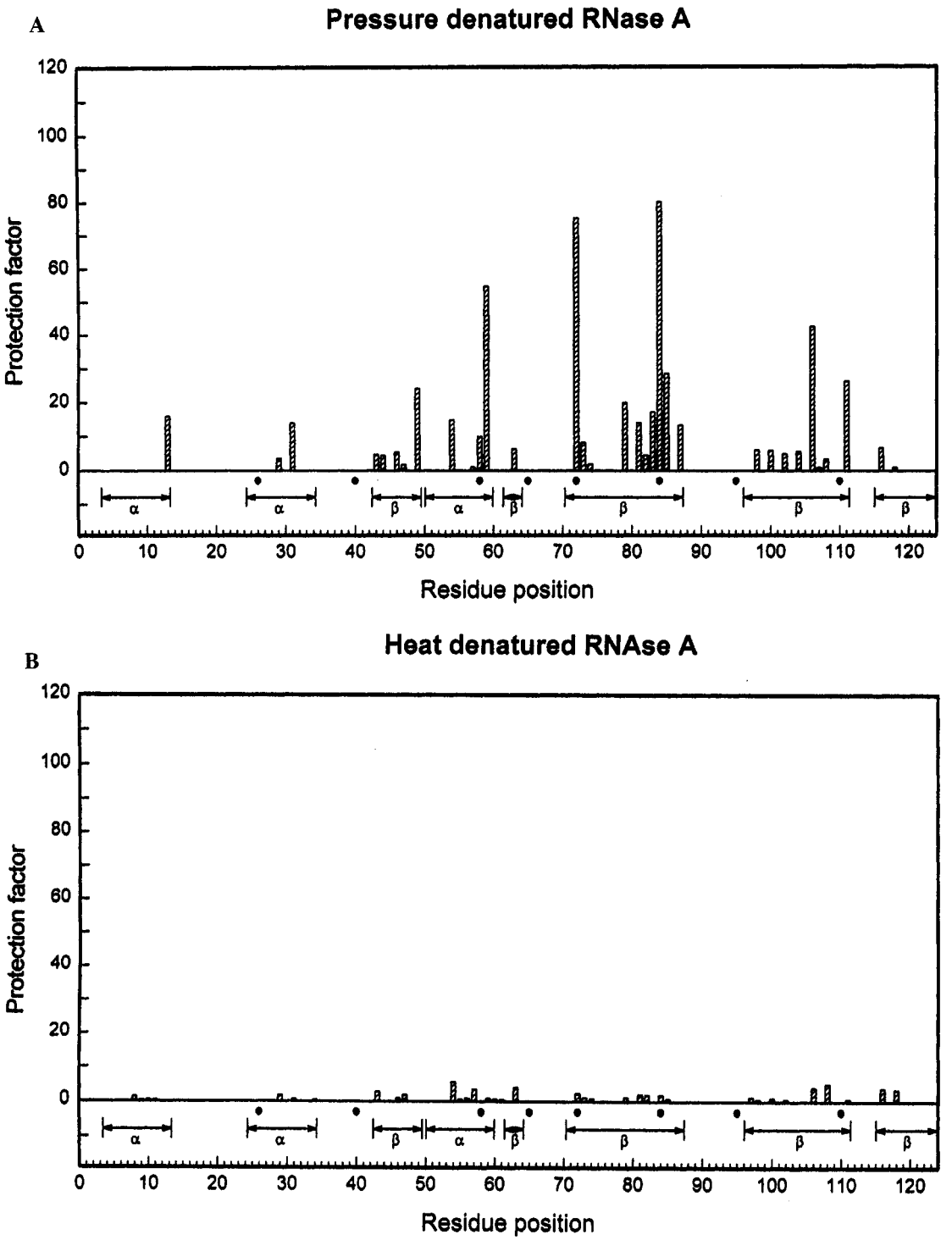

FIGURE 10: Comparison of the protection factors for the amide proton exchange in the pressure-denatured and heat-denatured RNase A: (A) in the pressure-denatured state the protection factors *versus* the protein sequence; (b) in the heat-denatured state the protection factors *versus* the protein sequence. Data were reported by Robertson and Baldwin (1991); ●, cysteine residue.

(residues 3−12) partially uncoils first, and this region moves away from the main part of the protein. The movement of the N-terminal region residues (1−25) then induces the opening of the crevice; the region near His48 then can unravel. After that, the β-strand near the C-terminus begins to loosen from the β-sheet and is partially exposed to the solvent. Finally, some of the remaining structure of the protein further unfolds; however, the structure of the pressure-denatured protein is far from completely unfolded.

It is interesting to find by 1D ^{1}H NMR spectra that a hydrogen-bonded helical structure exists around His12 of the pressure-denatured protein. Brown and Klee (1971) found by circular dichroism that the N-terminal peptide 1−13 of RNase A becomes partially helical at low temperature and high salt concentrations. It was reported that even the fully reduced RNase A has the tendency to adopt local nonrandom conformations, especially a helical conformation near the N-terminus (Haas et al., 1988; Osterhout et al., 1989). The *S*-peptide study by Blum et al. (1978) is consistent with Brown and Klee's results and confirms that the N-terminal α-helix of RNase A is an intermediate in folding. One significant finding of this work is that the pressure-denatured state of RNase A at low pH retains a partially folded structure, e.g., it contains the native-like helical structure

found near the N-terminal end of native RNase A. In addition, it seems reasonable to assume that the structure of pressure-denatured RNase A resembles that of the early intermediate found by Blum et al. (1978) in the temperature-jump experiment. It has been pointed out recently that the residual structures, such as those found in the pressure-denatured state, may resemble folding intermediates or serve as initiation sites for protein folding (Wright et al., 1988; Moult & Unger, 1991).

It has been proposed that conformational fluctuations play an important role in the structure of globular proteins (Cooper, 1976; Gekko & Noguchi, 1979; Gekko & Hasegawa, 1986). With increasing pressure, the native conformation of a protein is distorted, the protein structure becomes more flexible, and the volume fluctuation of the protein increases. The increased volume fluctuation may produce cavities or channels in some areas of the protein. Therefore, with the assistance of pressure, water molecules are able to penetrate into the hydrophobic core of a protein. This results in the exposure of much more of the inner surface to solvent molecules and disrupts the native structure of the protein. This volume fluctuation argument is supported by the experimental results of the RNase A−inhibitor complex under high pressure. The hydrogen-bonding interaction between the protein and the inhibitor can reduce the volume fluctuation. Therefore, the interaction stabilizes the whole protein structure instead of only the active site of the protein. The pressure-denatured RNase A adopts a compact structure under high pressure; the volume fluctuation of the protein increases by about 10% upon pressure denaturation compared to that of the native protein (Brandts et al., 1970; Gekko & Hasegawa, 1986).

The hydrogen-exchange technique has been applied to a variety of conformational states of proteins, including partially folded states under equilibrium conditions and transient kinetic intermediates formed during the folding process (Englander, 1992; Baldwin, 1993; Matthias, 1994). A number of proteins in molten globular states show significant deviations in rates of hydrogen exchange from the random coil behavior, indicating that a significant amount of secondary or higher order structure remains in molten globular states. Udgaonkar and Baldwin (1988, 1990) studied the refolding of RNase A using pH pulse labeling hydrogen exchange. Their results reveal the complexity of the folding intermediates of the protein. No equilibrium molten globular conformation of RNase A that shows protection against hydrogen exchange was found in their experiments. The thermally unfolded RNase A at low pH shows some properties of a molten globule, and far-UV CD and FTIR spectra suggest that some secondary structure exists in the thermally unfolded state. However, no significant protection for any NH proton was found in the thermally denatured RNase A (Robertson & Baldwin, 1991). The results of the hydrogen-exchange experiments shown in Figure 10 can only be interpreted in a qualitative way, as more detailed high-pressure studies of the exchange process on model systems are needed. However, even if the k_{rc} values obtained from eq 4 must be regarded as a first approximation, we have no reason to expect that this calculation would lead to an erroneous pattern of the protection factors in the pressure-denatured state. It is also important to note that the pattern of protection coincides with secondary structures of the native protein. The fact remains that, so far, all experimental evidence (Jonas & Jonas, 1994) indicates that the pressure-denatured states of proteins have more secondary structure than temperature- and urea-denatured states.

From our exploratory high-pressure hydrogen-exchange experiment, we can only conclude that the pressure-denatured state of ribonuclease A contains come partial secondary structure, in contrast to its thermally denatured state, which contains little or no stable hydrogen-bonded structure (Robertson & Baldwin, 1991). In interpreting high-pressure data, one has to fully appreciate the complexity of pressure effects as one changes water−water interactions, water−protein interactions, and protein−protein interactions. It was pointed out (Bai et al., 1993) that the H-exchange rates can be significantly influenced by neighboring side chains even in the absence of a folded structure. Clearly, one cannot rule out that the pressure may influence the steric blocking effects in pressure-denatured states. Nevertheless, the high-pressure exchange experiments appear promising, and therefore, systematic high-pressure studies of hydrogen exchange on simple amide and polyamide systems are in progress. We expect that the availability of such fundamental high-pressure experimental data dealing with hydrogen exchange will enable interested workers to draw more quantitative conclusions when interpreting high-pressure hydrogen-exchange experiments of the type performed in this study. Keeping in mind the caveat regarding the approximate nature of the calculation of k_{rc} at high pressure, we want, nevertheless, to point out some of the distinct features of the pattern of the protection factors as shown in Figure 10. In the present work, we find that in the pressure-denatured RNase A most of interior amide groups exchange hydrogen atoms with the solvent more rapidly than in the folded state, but more slowly than in the fully unfolded state. Clearly, at least some secondary structure, which is more or less native, seems to persist in the pressure-denatured state to protect the NH hydrogens from exchange with solvent molecules. The pressure-denatured state appears to display some characteristics of a molten globule or compact intermediate, which is a collapsed molecule with native-like secondary structure and a liquid-like interior (Ptitsyn, 1987; Kim & Baldwin, 1990).

The kinetic folding intermediate of RNase A was found in the early stage of refolding by pulsed hydrogen exchange (Udgaonkar & Baldwin, 1988, 1990). All NH protons that are hydrogen-bonded within the β-sheet of native RNase A are protected in the intermediate. During folding, the β-sheet is formed rapidly and cooperatively and becomes more stable with time. It is interesting to note that the NH protons near the center of the β-sheet (residues 70−87) of native RNase A are more strongly protected, with an average protection factor above 25, while the average protection factors of the other β-strand are between 4 and 12. On the other hand, the average protection factor of the β-strand close to the C-terminus of native RNase A is very low ($\sim$4) compared to those of other parts of the protein. It also can be seen in Figure 10 that the protection factors of the peptide bonds in the C-terminal β-strand decrease along the sequence toward the end. In accord with these observations, we may conclude that, for pressure-denatured RNase A, hydrogen exchange is slower in the center of the β-sheet of the native protein than at the end; the β-strand close to the C-terminus of native RNase A is more unfolded and more flexible than the β-strand near the center of the β-sheet. It is very possible that the β-strand in the interior of the native protein (residues 70−87) is also part of the hydrophobic core of the protein

in the pressure-denatured state. It is interesting to note that some of the residues with large protection factors ($P > 50$) are those near the disulfide bonds. Obviously, the covalent disulfide bonds cannot be broken by the high pressure used in the experiment, and all four pairs of disulfide bonds stabilize adjacent structures and protect against solvent exchange.

Privalov (1990) proposed that cold denaturation is a general phenomenon caused by the very specific and strongly temperature-dependent interaction of nonpolar protein groups with water. During cold denaturation, the Gibbs energy of hydration is negative and increases in magnitude as temperature decreases. Therefore, proteins expose their internal groups to water and unfold at sufficiently low temperautres. Our cold denaturation of RNase A, as well as of lysozyme and myoglobin (unpublished results), demonstrates the fact that, by varying temperature and pressure and adjusting pH, globular proteins can be cold-denatured in aqueous solutions. However, conformations of cold-denatured proteins appear to be quite different from those of heat-denatured states. The cold-denatured proteins have a more compact structure and may contain large amounts of secondary or higher order structures. More detailed information on the cold-denatured structures of proteins can be obtained by using pulsed hydrogen exchange and two-dimensional NMR techniques in the temperature- and pressure-jump experiments, and work along these lines on the cold denaturation of RNase A is in progress in our laboratory.

ACKNOWLEDGMENT

We thank Professor Peter Wolynes for his helpful comments. We also express our thanks to the referees for their constructive comments.

REFERENCES

Anfinsen, C. B. (1973) *Science 181*, 223−230.
Antonino, L. C., Kautz, R. A., Nakano, T., Fox, R. O., & Fink, A. L. (1991) *Proc. Natl. Acad. Sci. U.S.A. 88*, 7715−7718.
Aue, W. P., Bartholdi, E., & Ernst, R. R. (1976) *J. Chem. Phys. 64*, 2229−2246.
Bai, Y., Milne, J. S., Mayne, L., & Englander, S. W. (1993) *Proteins: Struct., Funct., Genet. 17*, 75−86.
Baldwin, R. L. (1993) *Curr. Opin. Struct. Biol. 3*, 84−91.
Benz, F. W., & Roberts, G. C. K. (1975a) *J. Mol. Biol. 91*, 345−365.
Benz, F. W., & Roberts, G. C. K. (1975b) *J. Mol. Biol. 91*, 367−387.
Biringer, R. G., & Fink, A. L. (1982) *Biochemistry 21*, 4748−4755.
Blum, A. D., Smallcombe, S. H., & Baldwin, R. L. (1978) *J. Mol. Biol. 118*, 305−316.
Brandts, J. F., Oliverira, R. J., & Westort, C. (1970) *Biochemistry 9*, 1038−1047.
Brown, J. E., & Klee, W. A. (1971) *Biochemistry 10*, 470−476.
Bryngelson, J. D., & Wolynes, P. G. (1987) *Proc. Natl. Acad. Sci. U.S.A. 84*, 7524−7528.
Bryngelson, J. D., & Wolynes, P. G. (1989) *J. Phys. Chem. 93*, 6902−6915.
Bryngelson, J. D., & Wolynes, P. G. (1990) *Biopolymers 30*, 177−188.
Bryngelson, J. D., Onuchic, J. N., Socci, N. D., & Wolynes, P. G. (1994) *Proteins: Struct., Funct., Genet.* (in press).
Carter, J. V., Knox, D. G., & Rosenberg, A. (1978) *J. Biol. Chem. 253*, 1947−1953.
Cook, K. H., Schmid, F. X., & Baldwin, R. L. (1979) *Proc. Natl. Acad. Sci. U.S.A. 76*, 6157−6161.
Cooper, A. (1976) *Proc. Natl. Acad. Sci. U.S.A. 73*, 2740−2741.
Covington, A. K., Robinson, R. A., & Bates, R. G. (1966) *J. Phys. Chem. 70*, 3820−3824.
Creighton, T. E. (1990) *Protein Folding*, W. H. Freeman & Co., New York.
Creighton, T. E. (1993) *Proteins*, W. H. Freeman & Co., New York.
Crook, E. M., Mathias, A. P., & Rabin, B. R. (1960) *Biochem. J. 74*, 234−238.
Dobson, C. M., & Evans, P. A. (1984) *Biochemistry 23*, 4267−4270.
Englander, S. W., & Mayne, L. (1992) *Annu. Rev. Biophys. Biomol. Struct. 21*, 243−265.
Evans, P. A., Kautz, R. A., Fox, R. O., & Dobson, C. M. (1989) *Biochemistry 28*, 362−370.
Franks, F., & Hatley, R. H. M. (1985) *Cryo-Lett. 6*, 171−180.
Gekko, K., & Noguchi, H. (1979) *J. Phys. Chem. 83*, 2706−2714.
Gekko, K., & Hasegawa, Y. (1986) *Biochemistry 25*, 6563−6571.
Glasoe, P. F., & Long, F. A. (1960) *J. Phys. Chem. 64*, 188−193.
Haas, E., McWherter, C. A., & Scheraga, H. A. (1988) *Biochemistry 27*, 1−21.
Hatley, R. H. M., & Franks, F. (1986) *Cryo-Lett. 7*, 226−233.
Howarth, O. W. (1979) *Biochim. Biophys. Acta 576*, 163−175.
Jonas, J. (1982) *Science 216*, 1179−1884.
Jonas, J. (1987) *NATO ASI Ser. C 41*, 193−236.
Jonas, J., & Jonas, A. (1994) *Annu. Rev. Biophys. Biomol. Struct. 23*, 287−318.
Kim, P. S., & Baldwin, R. L. (1980) *Biochemistry 19*, 6124−6129.
Kim, P. S., & Baldwin, R. L. (1990) *Annu. Rev. Biochem. 59*, 631−660.
Kitamura, Y., & Itoh, T. (1987) *J. Solution Chem. 16*, 715−725.
Labhardt, A. M. (1982) *J. Mol. Biol. 114*, 181−293.
Matthias, B., Radford, S. E., & Dobson, C. M. (1994) *J. Mol. Biol. 237*, 247−254.
Moult, J., & Unger, R. (1991) *Biochemistry 30*, 3816−3824.
Osterhout, J. J., Baldwin, R. L., York, E. J., Stewart, J. M., Dyson, H. J., & Wright, P. E. (1989) *Biochemistry 28*, 7059−7064.
Peng, X., Jonas, J., & Silva, J. L. (1993) *Proc. Natl. Acad. Sci. U.S.A. 90*, 1776−1780.
Peng, X., Jonas, J., & Silva, J. L. (1994) *Biochemistry 33*, 8323−8329.
Petal, D. J., Canuel, L. L., & Bovey, F. A. (1975) *Biopolymers 14*, 987−997.
Privalov, P. L. (1990) *CRC Crit. Rev. Biochem. Mol. Biol. 25*, 181−305.
Ptitsyn, O. B. (1987) *J. Protein Chem. 6*, 273−293.
Rico, M., Bruix, M., Santorio, J., Gonzalez, C., Neira, J. L., Nieto, J. L., & Herranz, J. (1989) *Eur. J. Biochem. 183*, 623−638.
Robertson, A. D., & Baldwin, R. L. (1991) *Biochemistry 30*, 9907−9914.
Robertson, A. D., Purisma, E. O., Eastman, M. A., & Scheraga, H. A. (1989) *Biochemistry 28*, 5930−5938.
Royer, C. A., Hinck, A. P., Loh, S. N., Prehoda, K. E., Peng, X., Jonas, J., & Markley, J. L. (1993) *Biochemistry 32*, 5222−5232.
Samarasinghe, S. D., Campbell, D. M., Jonas, A., & Jonas, J. (1992) *Biochemistry 31*, 7773−7778.
Schmid, F. X. (1983) *Biochemistry 22*, 4690−4696.
Schmid, F. X., & Baldwin, R. L. (1979) *J. Mol. Biol. 135*, 199−215.
Seshadri, S., Oberg, K. A., & Fink, A. L. (1994) *Biochemistry 33*, 1351−1355.
Tamura, A., Kimura, K., & Akasaka, K. (1991) *Biochemistry 30*, 11313−11320.
Tsong, T. Y., Hearn, R. F., Wrathall, D. P., & Sturtevant, J. M. (1970) *Biochemistry 9*, 2666−2677.
Udgaonkar, J. B., & Baldwin, R. L. (1988) *Nature 335*, 694−699.
Udgaonkar, J. B., & Baldwin, R. L. (1990) *Proc. Natl. Acad. Sci. U.S.A. 87*, 8197−8201.
Weber, G., & Drickamer, H. G. (1983) *Q. Rev. Biophys. 16*, 89−112.
Westmoreland, D. G., & Matthews, C. R. (1973) *Proc. Natl. Acad. Sci. U.S.A. 70*, 914−918.
Wright, P. E., Dyson, H. J., & Lerner, R. A. (1988) *Biochemistry 27*, 7167−7175.
Zipp, A., & Kauzmann, W. (1973) *Biochemistry 12*, 4217−4228.

BI942805N